Alternating-Laser Excitation of Single Molecules

ACHILLEFS N. KAPANIDIS,*,†,‖
TED A. LAURENCE,*,†,‡ NAM KI LEE,†,§
EMMANUEL MARGEAT,†,⊥
XIANGXU KONG,† AND SHIMON WEISS*,†

Department of Chemistry and Biochemistry and Department of Physiology, University of California, Los Angeles, 607 Charles E. Young Drive East, Los Angeles, California 90095-1569, and Physical Biosciences Institute, Lawrence Livermore National Laboratory, Livermore, California 94551

Received July 7, 2004

ABSTRACT

Single-molecule fluorescence spectroscopy addresses biological mechanisms and enables ultrasensitive diagnostics. We describe a new family of single-molecule fluorescence methods that uses alternating-laser excitation (ALEX) of diffusing or immobilized biomolecules to study their structure, interactions, and dynamics. This is accomplished using ratios that report on the distance between and the stoichiometry of fluorophores attached to the molecules of interest. The principle of alternation is compatible with several time scales, allowing monitoring of fast dynamics or simultaneous monitoring of a large number of individual molecules.

Achillefs N. Kapanidis received his B.S. in chemistry (1991) from the Aristotelian University of Thessaloniki, Greece, and his M.Sc. (food chemistry, 1993) and Ph.D. (biological chemistry, 1999) from Rutgers University, New Jersey. Following postdoctoral research at Lawrence Berkeley National Laboratory, he became an Assistant Researcher in the Department of Chemistry and Biochemistry at UCLA. In late 2004, he joined the University of Oxford, United Kingdom, as a University Lecturer in Biological Physics. He studies protein—nucleic acid transactions using single-molecule spectroscopy and biochemistry.

Ted A. Laurence received his B.S. (1997) from California Institute of Technology. He was a National Science Foundation Graduate Fellow (1997—2000) and obtained his Ph.D. (2002) from the University of California, Berkeley. After postdoctoral research at UCLA, he became a fellow in the Physical Biosciences Institute at Lawrence Livermore National Laboratory. His interests include biological applications of single-molecule spectroscopy and surface-enhanced Raman spectroscopy.

Nam Ki Lee received his B.S. (1998) and M.Sc. (2000) from Seoul National University, South Korea. As part of his Ph.D., he joined UCLA (2002—2003) to study single-molecule spectroscopy and biochemistry. He continues this work as a Ph.D. candidate at Seoul National University.

Emmanuel Margeat received his B.S. in physical chemistry (1996) from the University Paul Sabatier in Toulouse, France, and his Ph.D. in biochemistry and molecular biology (2001) from the University of Montpellier, France. He next joined the group of Shimon Weiss at UCLA, studying single-molecule fluorescence methods. Since 2004, he has been a CNRS researcher, working on protein—nucleic acid interactions at the Centre de Biochimie Structurale, Montpellier.

Xiangxu Kong received his B.S. from Beijing University, China (2001). He is presently a Ph.D. candidate in physical chemistry at UCLA. He studies protein folding and protein—protein interactions using single-molecule fluorescence methods.

Shimon Weiss received his B.S. (1984) and D.Sc. (1989) in electrical engineering from Technion, the Israel Institute of Technology. He did his postdoctoral research at AT&T Bell Laboratories, New Jersey. In 1990, he became a Staff Scientist at Lawrence Berkeley National Laboratory, California. In 2001, he joined UCLA as a Professor of Chemistry and of Physiology. His research interests span the biophysics—chemistry—biology—medicine—nanotechnology interfaces.

Introduction

Room-temperature, real-time observation of individual molecules is revolutionizing several areas of physics, chemistry, and biology by eliminating the ensemble averaging present in conventional analysis and by uncovering static and dynamic heterogeneities.[1,2] Single-molecule methods monitor dynamics of biomolecules under equilibrium conditions and complex reaction kinetics under nonequilibrium conditions,[3] capturing views that are inaccessible to ensemble methods owing to the lack of synchronization of biomolecules.

Single-molecule detection is characterized by three major attributes. First, the properties of ensembles of billions of molecules can be described reliably by observations of a few single molecules (due to ergodicity). Second, single-molecule observations carry far more information than do ensembles (when ergodicity breaks down). Third, the amount of sample necessary to capture the new information is miniscule ($<10^{-16}$ mol), several orders of magnitude lower than the amount needed for ensemble methods. Such properties are well aligned with modern science, which moves toward smaller scales, higher throughputs, and higher-complexity systems, the descriptions of which require monitoring of several observables. However, to mine the wealth of information displayed by single molecules, one has to pose the "right" questions to the molecules; in the case of single-molecule fluorescence spectroscopy (SMFS),[4,5] this requirement led to novel fluorescent probes and labeling strategies[6] and complex excitation/detection schemes. SMFS is applied to either diffusing or immobilized molecules, accessing different time scales of information. Several excellent reviews exist on many aspects of SMFS.[7—15]

Here, we describe a new family of fluorescence methods that uses alternating-laser excitation of single molecules to study their structure, interactions, and dynamics through measurements of distances and stoichiometries.

Climbing the Ladder of Complexity: More Excitations, Fluorophores, and Emissions

The pioneers of SMFS were concerned with the milestones of detecting a single molecule and a single fluorophore. The first milestone was reached in 1976 by Hirschfeld, who detected single antibodies carrying ~100 fluorophores.[16] Fifteen years later, the Keller group at Los Alamos, driven by single-molecule DNA sequencing, detected single fluorophores in solution at room temperature[17] (cryogenic

* Corresponding authors. Phone numbers: (310) 794-0093 (S.W.); +44-1865-272-401 (A.N.K.); (925) 422-1788 (T.A.L.). Fax: +44-1865-282-208. E-mail addresses: a.kapanidis1@physics.ox.ac.uk; laurence2@llnl.gov; sweiss@chem.ucla.edu.
† University of California, Los Angeles.
‡ Lawrence Livermore National Laboratory.
§ Present Address: School of Chemistry, Seoul National University, Seoul, Korea 151—747.
‖ Present address: Department of Physics and IRC in Bionanotechnology, University of Oxford, Oxford, United Kingdom.
⊥ Present Address: Centre de Biochimie Structurale, CNRS, Montpellier, France.

detection of single molecules will not be discussed here). Room temperature observations of immobilized single fluorophores were followed by near- and far-field microscopies, with applications in biomolecular systems (reviewed in ref 4). Early methods employed a single excitation wavelength and a single emission wavelength to interrogate molecules labeled with a single fluorophore, reporting on fluorophore localization on a surface, fluorescence lifetime, diffusion constants, or changes in quantum yield.

Steps toward higher complexity introduced a second detection channel. The added channel detected a second polarization component or a different wavelength, reporting on the location and rotational freedom of fluorophores or on spectral jumps due to transient changes in emission spectra (reviewed in ref 4).

Soon thereafter, a second fluorophore was introduced; the presence of two fluorophores within a certain distance allowed interprobe distance measurements, either through high-resolution localization of the two fluorophores or through fluorescence resonance energy transfer (FRET; also known as Förster resonance energy transfer). In both cases, the use of single-wavelength excitation was maintained (Figure 1). An application of the single-excitation/multiple-emissions concept used semiconductor nanocrystals for ultrahigh-resolution colocalization,[18] since nanocrystals of different sizes combine overlapping, wide, high cross-section excitation bands with distinct, sharp emission bands (Figure 1A). Thus, nanocrystals of distinct emission bands were excited and detected simultaneously, enabling multicolor imaging.[19] A similar concept is employed for two-photon excitation of fluorophores.[20] Unlike the absorption spectrum for single-photon excitation (narrow and symmetric to the emission spectrum), two-photon excitation spectra are relatively wide and independent of emission wavelength (Figure 1B), permitting simultaneous excitation of distinct-emission fluorophores by a single far-red or infrared laser.

A breakthrough in our ability to monitor structure and interactions occurred in 1996, when FRET between a single pair of fluorophores (single-pair FRET; spFRET) was demonstrated. FRET is the nonradiative transfer of excitation energy from a fluorophore serving as a donor (D) to a complementary fluorophore serving as an acceptor (A). FRET acts as a "spectroscopic ruler" for the $1-10$ nm scale, since FRET efficiency, E, is a sensitive function of interprobe distance R (specifically, $E = [1 + (R/R_0)^6]^{-1}$, where R_0 is a constant that equals the interprobe distance at $E = 50\%$). Initial work was followed by far-field observations, both for molecules immobilized on surfaces[21] and for those diffusing in solution.[22] The development of spFRET was a pivotal moment for single-molecule detection; it paved the way for studying macromolecular structure and interactions and has been used to study the dynamics of proteins, nucleic acids, and their complexes,[2,12] mainly by observing distance changes and their kinetics.

However, during mechanistic analysis of transcription complexes by our group, it became apparent that spFRET was not a *general* platform for quantitative analysis of
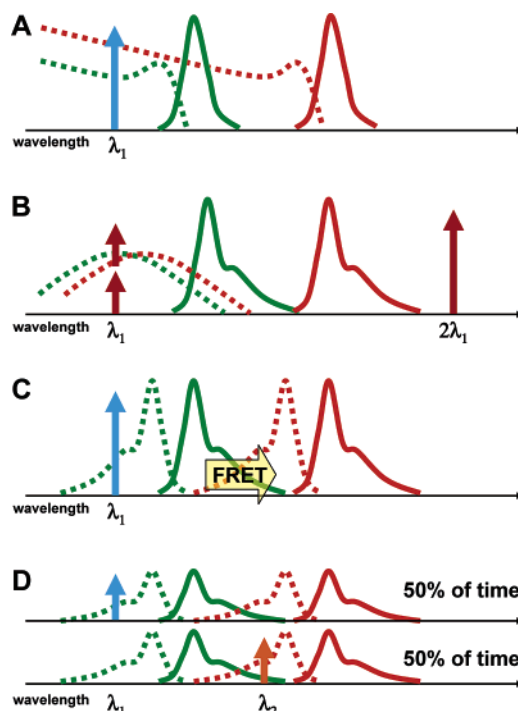
FIGURE 1. Single- and alternating-laser excitation approaches to SMFS: (A) single-laser excitation of fluorophores with wide overlapping excitation spectra and separable emission spectra; (B) single-laser excitation of fluorophores with wide overlapping two-photon excitation spectra and separable emission spectra; (C) single-laser excitation of fluorophores participating in FRET in which the donor is excited *directly* by the laser and emits at the D-emission wavelength whereas part of the D-excitation energy is transferred to the acceptor, which emits at wavelengths longer than the donor; (D) alternating-laser excitation of fluorophores able to participate in FRET. For 50% of the time, the donor is excited by the D-excitation laser; in the case of FRET, there is acceptor emission. For the rest of the time, the acceptor is excited by the A-excitation laser, resulting in A-emission. Duty cycles can vary.

structure, due to numerous corrections required to measure FRET accurately and to the presence of species that obscure FRET measurements when $R > 6-8$ nm. Moreover, spFRET is not a *general* platform for quantitative analysis of interactions. For example, for the interaction $M^A + L^D \rightleftharpoons M^A L^D$ (where M^A is an acceptor-labeled macromolecule and L^D is a donor-labeled ligand), spFRET cannot quantitate the major species involved owing to several factors: First, spFRET yields a measurable signal only when D–A distances in the $M^A L^D$ complex are sufficiently short ($R_{D-A} < 6-8$ nm) to distinguish complexes from free L^D species. Second, inactive states of acceptors result in ML^D species that exhibit D-only characteristics,[22] leading to apparent increases in free L^D species. Finally, no M^A species are detected, and complexes with stoichiometries other than 1:1 (e.g., $M^A[L^D]_2$) cannot be identified as such by spFRET. These limitations, compounded with substoichiometric labeling, photophysics, photobleaching, and aggregation/dissociation phenomena, have limited the implementation of spFRET and called for additional observables to improve its resolving capability.

All methods described up to this point use single excitation sources, mainly to avoid chromatic aberrations

(such as different *z* focus and point-spread function diameters for pointlike objects[18]) associated with multi-wavelength excitation. While such limitations of multi-wavelength excitation are relevant for ultrahigh-resolution colocalization, they do not affect correlation- or ratio-based measurements, where such differences are normalized. This is true for dual- or triple-color fluorescence cross-correlation spectroscopy, which employs multi-wavelength excitation of multicolor samples combined with multichannel detection. Dual-wavelength excitation was also applied to single molecules to perform coincidence analysis and to determine interaction stoichiometries;[23] however, only a small fraction (~30%) of the molecules were excited by both lasers because of imperfect overlap of their focal volumes. The multiwavelength approach has not been applied to spFRET, since extraction of accurate FRET is complicated by uncertainty over the source of acceptor-emission photons (i.e., photons due to FRET vs those due to direct acceptor excitation).

In conclusion, proximity between a FRET donor and acceptor is necessary for distance analysis but insufficient for interaction analysis; on the other hand, coincidence of a FRET donor and acceptor in the absence of FRET is necessary for interaction analysis but generates no distance constraints.

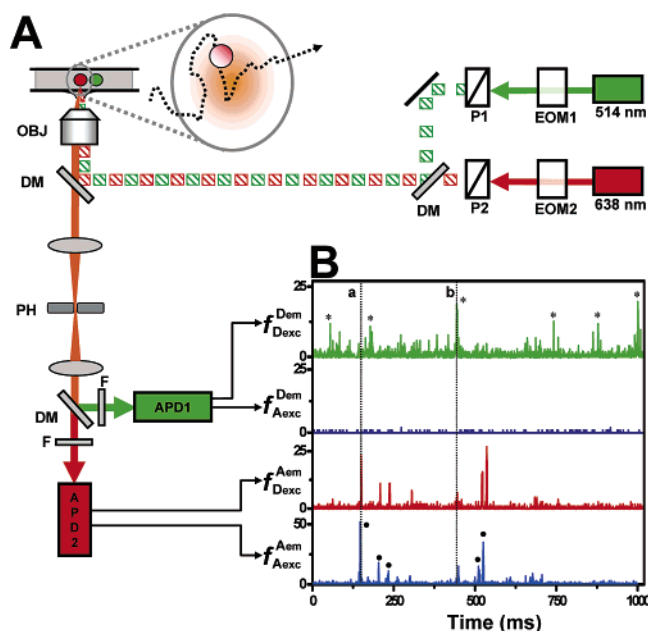## Alternating-Laser Excitation of Single Molecules

To develop a *general* FRET-based method for monitoring structure and interactions simultaneously, we reasoned that alternation between two excitation wavelengths accesses structural information using a donor-excitation wavelength and interaction information using both the donor- and acceptor-excitation wavelength. Thus, we introduced alternating-laser excitation (ALEX) spectroscopy,[24] a method that obtains D-excitation- and A-excitation-based observables for *each single molecule* by rapid switching between excitations[18] (Figure 2). Alternating excitation was used previously for immobilized molecules[25,26] but only as a qualitative check of acceptor presence.

Alternating excitation recovers distinct emission signatures (Figure 3A) by calculating two fluorescence ratios: the FRET efficiency, *E*, which reports on donor–acceptor distance,[22] and the distance-independent ratio, *S*, which reports on donor–acceptor relative stoichiometry:

$$E = F_{D_{exc}}^{A_{em}} / (F_{D_{exc}}^{A_{em}} + \gamma F_{D_{exc}}^{D_{em}})$$

$$S = F_{D_{exc}} / (F_{D_{exc}} + F_{A_{exc}})$$

where $F_{D_{exc}}^{D_{em}}$ is D-excitation-based D-emission, $F_{D_{exc}}^{A_{em}}$ is D-excitation-based A-emission, $F_{D_{exc}}$ is a sum of D-excitation-based emissions, $F_{A_{exc}}$ is a sum of A-excitation-based emissions (Figure 2B), and γ is a detection-correction factor.[21,22,24] All emissions refer to single molecules.


FIGURE 2. Alternating-laser excitation microscopy: Panel A shows an ALEX microscope: EOM = electrooptical modulator; P = polarizer; DM = dichroic mirror; OBJ = objective; PH = pinhole; F = filter; APD = avalanche photodiode. Modulators combined with polarizers result in alternating-laser excitation. After spatial and spectral filtering, fluorescence photons are detected on APDs. Panel B shows time traces for a high-FRET species. Fluorescence rates for the emission streams are represented as $f_{X_{exc}}^{Y_{em}}$ (emission rate in Y-emission detection channel while X-excitation laser is on). Burst "a" is a high-*E* D–A molecule; burst "b" is a D-only molecule. Dots indicate D–A species; asterisks indicate D-only species.

Stoichiometry *S* provides information even without close proximity between fluorophores; it allows thermodynamic and kinetic analysis of interactions, identification of interaction stoichiometry, and study of local environment. Two-dimensional *E*–*S* histograms (Figure 3A) allow virtual molecule-sorting; we define this analysis as fluorescence-aided molecule sorting (FAMS) and its implementation using alternating-laser excitation as ALEX-FAMS. When applied on diffusing molecules, ALEX-FAMS is a homogeneous (no washing), "mix-and-read" assay, in which optical readouts report *simultaneously* on the association and conformation status of single molecules.

Laser alternation is compatible with various time scales, since alternation periods can span three distinct time scales: the nanosecond time scale (using interlaced pulsed laser sources), the microsecond time scale (using continuous-wave lasers, modulators, and polarizers), and the millisecond time scale (combining microsecond-type sources and optics with wide field detection). The format is determined by the time scale of the process in question, the equilibrium/nonequilibrium nature of the measurement, and the observation time available (limited by diffusion or photobleaching).

Microsecond ALEX (*μ*s-ALEX): Structure and Interactions of Diffusing Molecules

We applied ALEX to diffusing molecules using microsecond time scale alternation (*μ*s-ALEX; Figure 3) using DNA
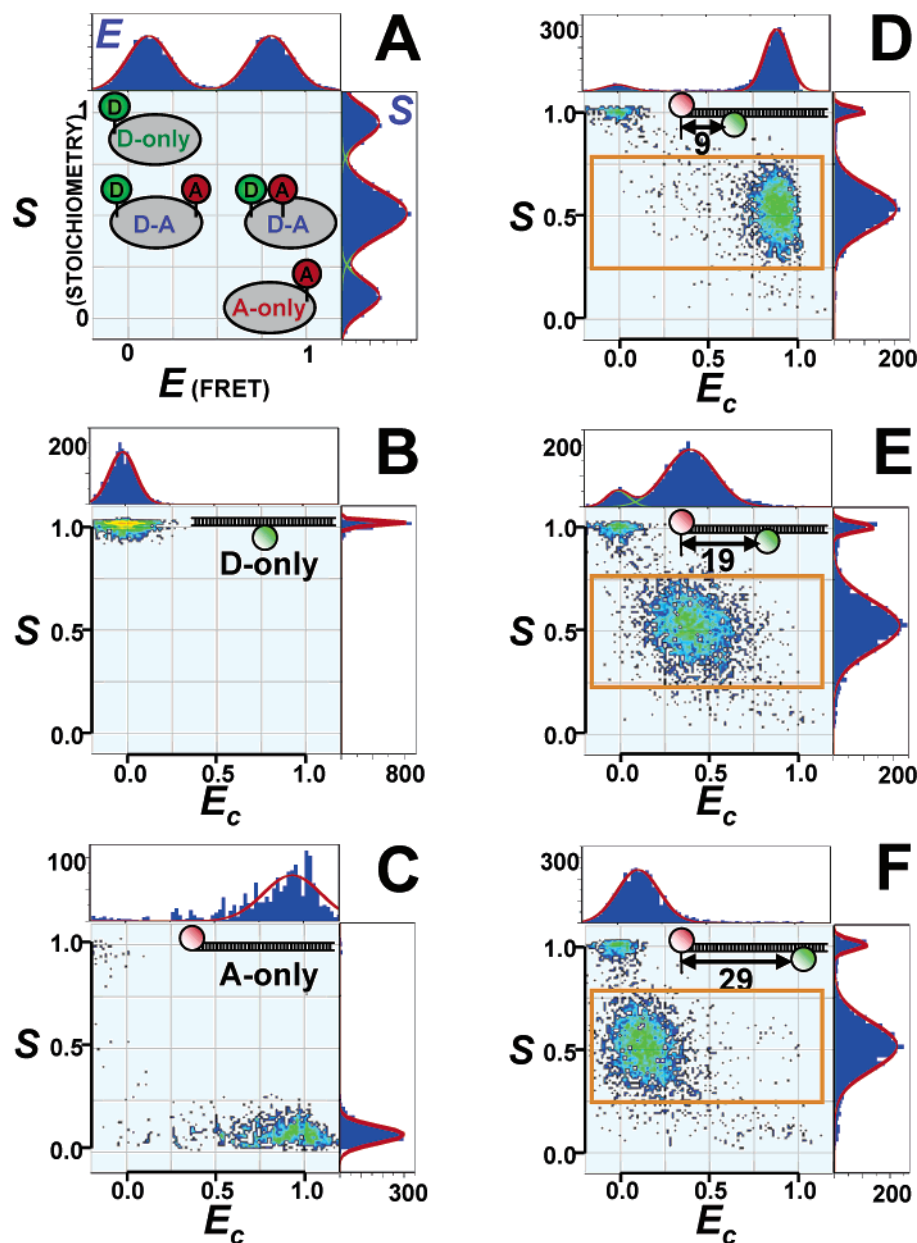
FIGURE 3. Sorting molecules using ALEX-FAMS. Panel A shows an E–S histogram for D-only, A-only, and D–A species with different interprobe distance, R_{D-A}. Ratio E sorts species according to FRET, reporting on structure; ratio S sorts species according to donor–acceptor stoichiometry, reporting on interactions. Sorting is also possible using one-dimensional histograms (red line = sum of fits; green line = individual fits). Although not required for sorting, we adjusted the excitation intensities of the two lasers to obtain $S \approx 0.5$ for D–A species (see Web Supplement 1 of ref 24). Panel B shows D-only DNA. Panel C shows A-only DNA. Panel D shows high-E DNA. Panel E shows intermediate-E DNA. Panel F shows low-E DNA.

fragments as D-only controls, A-only controls, and D–A species with various interprobe distances. On E–S histograms, D-only species appeared as species with low E and high S, whereas A-only species appeared as species with low S. In contrast, all D–A species displayed intermediate S and variable E (due to different D–A distance); the latter observation demonstrated the independence of E and S.

Since ALEX identifies D-only, A-only, and D–A species, it is suitable for analysis of interactions. In a binding equilibrium, D-only and A-only species represent free interactants and D–A represents a complex (Figure 4A); equilibrium binding and kinetic rate constants can be measured by counting molecules, due to the linear rela-

tion between observed molecules and concentration (for subnanomolar concentrations).[24] For an interaction of a macromolecule M^A with a ligand L^D (Figure 4A), which has an equilibrium dissociation constant K_d, the fraction of bound macromolecules (fractional occupancy θ) at ligand concentration [L] is $\theta = [ML]/([ML]+[M]) = [L]/([L] + K_d)$, transformed to

$$\theta = [D-A]/([D-A] + [A\text{-only}]) = [D\text{-only}]/([D\text{-only}] + K_d)$$

Measuring θ at several ligand concentrations $[L^D]$ allows calculation of K_d; θ can also be used to evaluate association/dissociation kinetics.
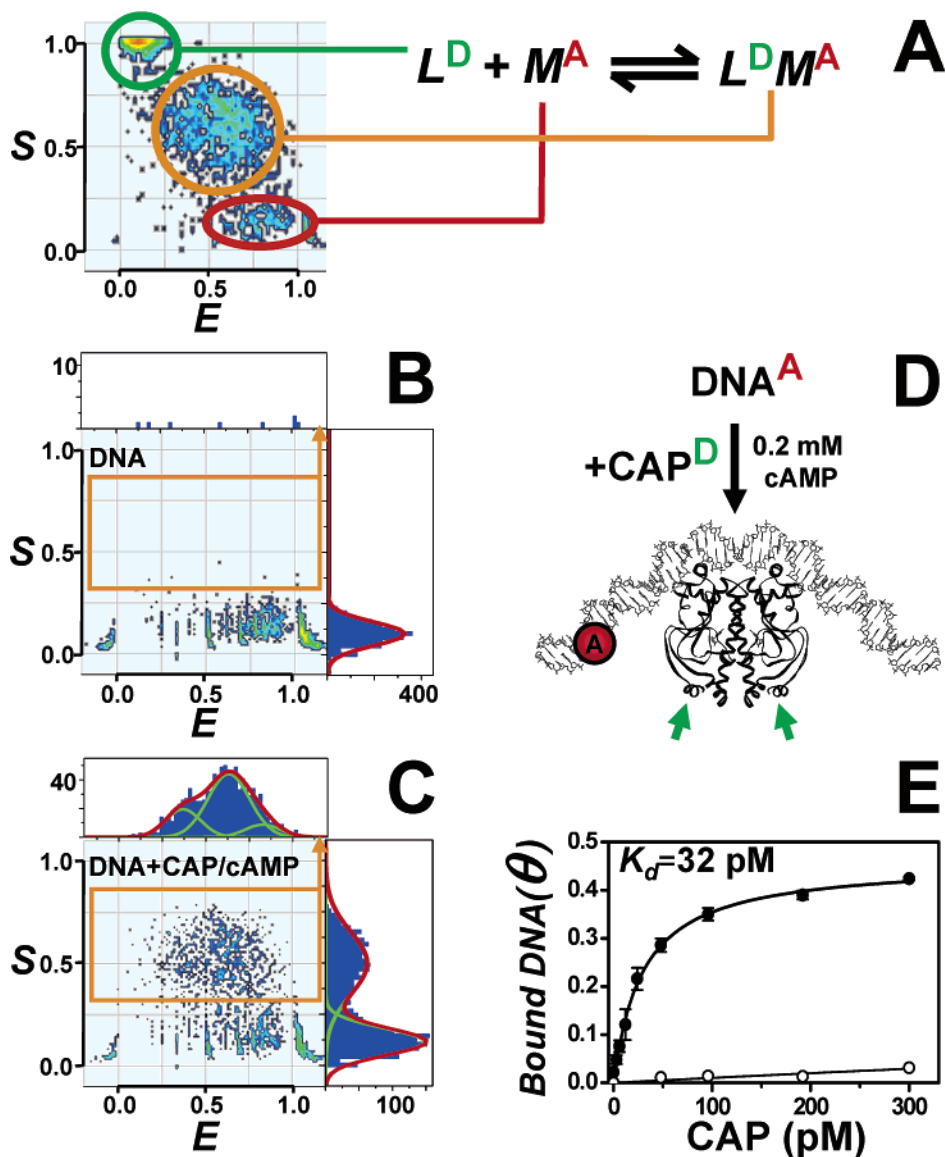
FIGURE 4. Analysis of protein–DNA interactions using ALEX-FAMS. Panel A shows analysis of interactions. Using a labeled macromolecule (M^A; A-only species) and a labeled ligand (L^D; D-only species), we can monitor the formation of complex $M^A L^D$ (D–A species) on the E–S histogram by monitoring occupancy, θ, at a ligand concentration, $[L^D]$. Panel B shows the E–S histogram for DNA^A. Panel C shows the E–S histogram for DNA^A, CAP^D, and cAMP. Panel D shows the CAP–DNA complex and labeling scheme. The acceptor was on DNA, and the donor on either of two possible sites on CAP (arrows); labeling efficiency was kept low, so most D–A species have one donor. The low labeling efficiency does not affect the determination of the binding constant of the interaction; it only changes the maximum occupancy, θ_{max}. Panel E shows titrations of DNA with CAP in the presence of cAMP (●, tight interaction) or in the absence of cAMP (○, weak interaction).

We studied the interaction of catabolite activator protein (CAP) with DNA as a model for protein–nucleic acid interactions by monitoring the interaction of D-labeled CAP (as "ligand" CAP^D; Figure 4D) with its preferred DNA site (as "macromolecule" DNA^A) with or without cyclic AMP (cAMP). With cAMP, CAP^D–DNA^A complexes were detected as D–A species (Figure 4C). CAP^D–DNA^A complexes displayed an E distribution with high E values (due to DNA bending toward CAP) and considerable heterogeneity (due to two possible D-labeling sites on CAP [Figure 4D] and interconversion between complexes with variable DNA bending). Without cAMP, few complexes were formed. We then assessed equilibrium binding by titrating DNA^A with CAP^D (Figure 4E). With cAMP, $K_d \approx 32$ pM; without cAMP, CAP binds to DNA >150-fold more weakly ($K_d > 5$ nM). Our analysis was in excellent agreement with ensemble assays.[24]

Accurate FRET Determination within Single Molecules Using ALEX

Since diffusion spFRET combines high sensitivity, the absence of surface-induced perturbations, and the ability to identify subpopulations, it is suitable for structural analysis of biomolecules with substantial heterogeneity. We demonstrated previously that diffusion spFRET can be used to measure distances within DNA.[22] However, due to limitations, spFRET had been confined to qualitative studies of structure and structural changes and to a FRET range between 40% and 100%.[22,27]
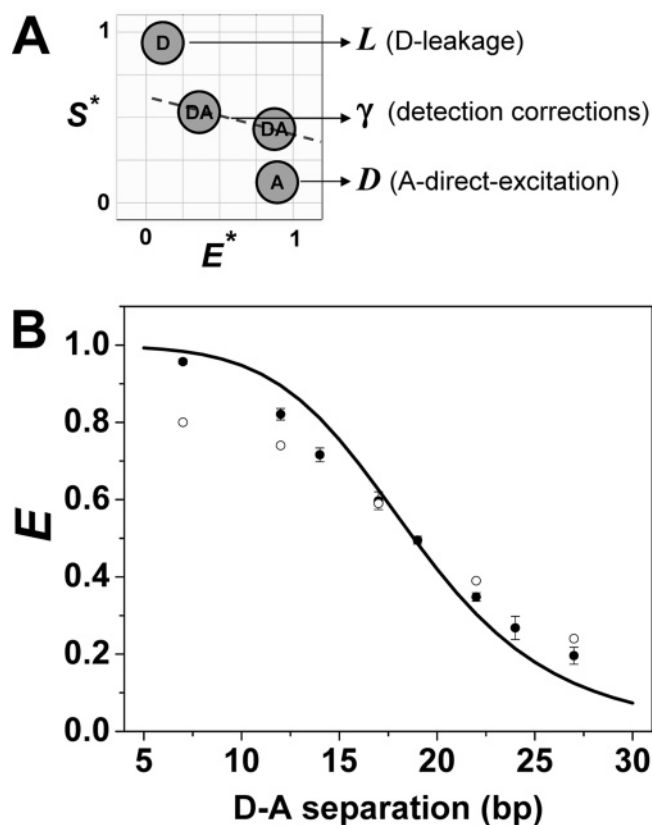
FIGURE 5. Accurate-E measurements using ALEX. Panel A shows sorted species (on E^*−S^* histograms; the asterisks denote modified expressions of E and S) required for recovering all correction factors needed for accurate-E measurements. D-only species provide D-leakage factor l (which accounts for D-emission into the A-detection channel), A-only species provide A-direct-excitation factor d (which accounts for A-emission into the A-detection channel due to A-direct-excitation by D_{exc}, and *not* due to FRET), and two or more D−A species with large difference in E provide the γ factor. Panel B shows comparison of corrected E values for DNA fragments featuring increasing donor−acceptor separation with predictions from a model of DNA: (●) FAMS-based E values (E_{sm}); (○) E from ensemble (E_{ens}).[29]

We recently used μs-ALEX to measure accurate FRET and distances from single molecules.[28] Using ALEX to sort species based on donor−acceptor distance and stoichiometry, we determined the correction factors needed for accurate FRET efficiencies (Figure 5A); such factors account for cross-talk terms contaminating the FRET-induced acceptor emission and for differences in the detection efficiency and quantum yield of the fluorophores. Since the correction factors were obtained directly and simultaneously with FRET efficiencies, ALEX-based distances were independent of instrument-specific factors, such as excitation intensity or detector alignment.

Using DNA fragments, we showed that ALEX-based distances agree with theoretical predictions from a simple cylindrical model of DNA helix[29] (Figure 5B); ALEX-based distances fit better to theory than distances obtained for the same fragments at the ensemble level. Measurements within large complexes yielded distances in excellent agreement with ensemble-FRET measurements and with models based on ensemble-FRET restraints and X-ray

crystallography. ALEX can complement structural analysis of biomolecules and their complexes, especially for species intractable by conventional structural biology due to excessive heterogeneity, limited stability, large size, presence of flexible domains, or transient nature.

## μs-ALEX Studies of Gene Transcription

Since ALEX monitors structure and interactions simultaneously, it can dissect biological processes orchestrated by coordinated changes in distance, stoichiometry, or both, such as binding events followed by conformational changes, translocation events on linear tracks culminating in dissociation of components, assembly/disassembly pathways, and template-directed oligomerization events.

We used ALEX to address questions about gene transcription, during which genes are copied to messenger RNA by the enzyme RNA polymerase (RNAP) (Kapanidis et al., manuscript in preparation). We first investigated the fate of initiation protein σ^{70} during the transition from transcription initiation to elongation, a transition known as promoter escape (where a promoter is a special DNA sequence that precedes genes).[30] Protein σ^{70} is required for RNAP binding to promoters, for opening double-stranded DNA to expose genetic information, and for disengaging RNAP from promoter DNA during escape. The textbook version of transcription predicts that 100% of σ^{70} dissociates after escape, but recent studies revealed σ^{70}-containing elongation complexes.[30]

An ALEX assay that addresses σ^{70} release uses a labeling scheme wherein a donor is placed on σ^{70} near the RNAP leading edge and an acceptor is placed at the downstream end of DNA and at a distance from the donor that results in low FRET; this scheme results in distinct outcomes for the two models describing the fate of σ^{70} upon escape (Figure 6A). Upon formation of the open RNAPσ^{70}−DNA complex (a complex wherein RNAP interacts with partly single-stranded promoter DNA and where no transcription occurs), two populations are seen (Figure 6B, left): free DNA (low-S species) and open complex (intermediate-S, low-E species). Under conditions that allow the formation of the first stable elongation complex by the large majority of open complexes,[30] no change is seen in the ratio of free DNA to RNAPσ^{70}−DNA complex (monitored by the S histogram), showing no dissociation of σ^{70} upon escape (Figure 6B, right). However, as seen in the E histogram for the RNAPσ^{70}−DNA complex, the donor−acceptor distance has decreased (compared with open complex), consistent with downstream translocation of RNAPσ^{70} on DNA. Using ALEX, we measured the content of σ^{70} in early and mature elongation complexes and studied their structure, stability, and dynamics, providing strong support for the proposal that σ^{70} release upon escape is not obligatory.

Millisecond-ALEX: Sorting Photophysics from Dynamics

To study dynamics in nonequilibrium systems, extended observations of individual molecules are necessary,
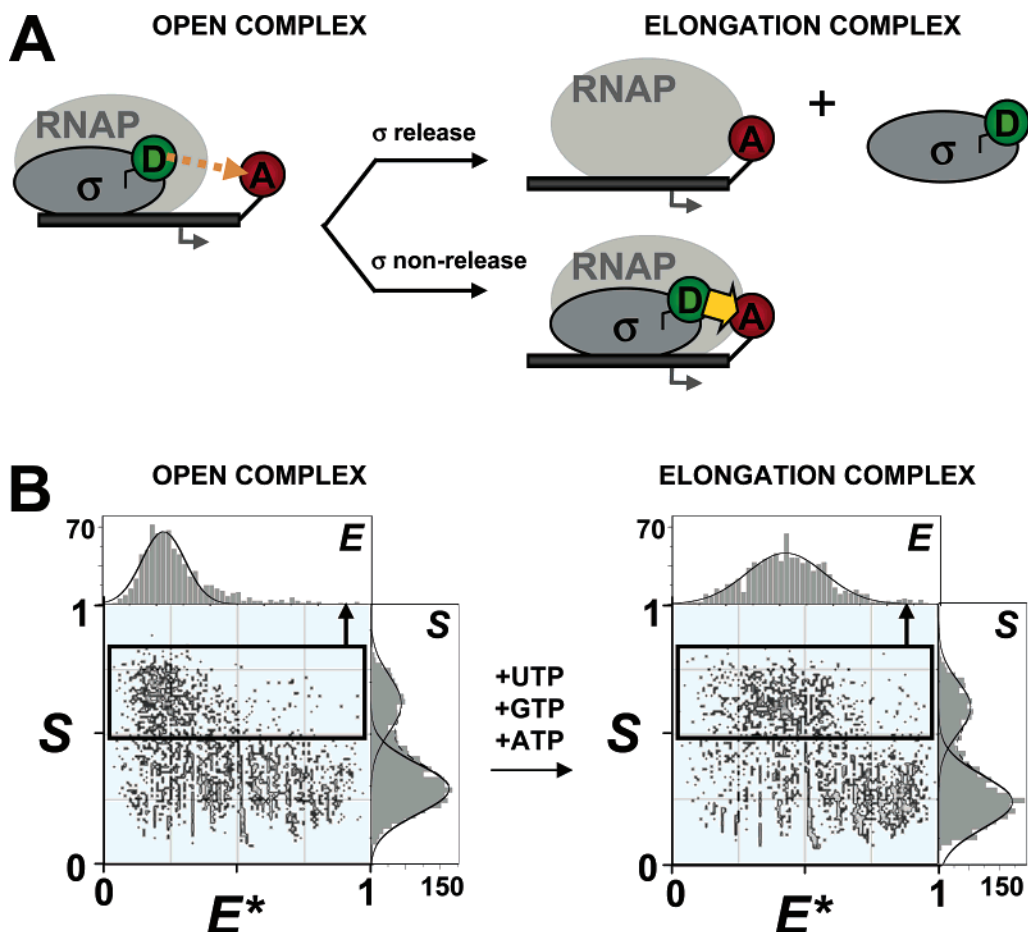
FIGURE 6. Application of ALEX to σ^{70} release upon promoter escape. Panel A presents predictions of models regarding σ^{70} release. Release of σ^{70} from an RNAP–DNA complex results in dissociation of a low-E D–A species to free σ^{70} (D-only) and to a σ-free RNAP–DNA elongation complex (A-only). In contrast, retention of σ^{70} converts a low-E^* D–A species to a high-E^* D–A species. Panel B presents E–S histograms for open and elongation complexes for promoter *lac*UV5 (E^* is a modified expression of E). Species with $0.45 < S < 0.8$ (D–A species; in black rectangle) correspond to σ^{70}-containing complexes with DNA, while species with $S < 0.3$ (A-only species) do not contain σ^{70}. The D–A species and A-only species are clearly separated on the S histogram. Since the S distribution remains unchanged upon formation of the first stable elongation complex, σ^{70} is retained upon escape.

achieved through simultaneous observation of multiple surface-immobilized molecules within a field of view. This is accomplished using total internal reflection (TIR) microscopy,[31] which combines evanescent-wave excitation within a thin layer from a surface and wide-field detection by an ultrasensitive camera.[12,32] However, single-excitation TIR suffers from limitations similar to those described earlier: the presence of artifactual D-only species, the inability to detect D–A species when $R_{D–A} \gg R_0$, the inability to detect A-only species, and complex photophysics.

To overcome such limitations, we combined ALEX with TIR microscopy in an approach termed as millisecond-ALEX (ms-ALEX) microscopy (Margeat et al., manuscript in preparation). The term *millisecond* refers to both detection and excitation time scales; it is, however, set by the frame rate of the camera, which is limited by the signal-to-noise ratio achieved using fluorophores compatible with single-molecule detection. The alternating-excitation source was formed as in μs-ALEX and sent to a prism-based TIR microscope.[31] Donor and acceptor fluorescence was detected using dual-view detection[33] (four emission intensities per molecule; Figure 7A), and ratios

E and S were calculated for each molecule and at each alternation period.

ms-ALEX was tested on surface-immobilized transcription complexes, achieving specific immobilization by preparation of biotinylated complexes, surface modification with biotin–poly(ethylene glycol) and streptavidin, incubation of complexes with the modified surface, and wash of unbound material.[32] After analyzing minute-long movies, we constructed E–S histograms that resolve D-only (high-S, low-E), A-only (low-S), and D–A (intermediate-S) species (Figure 7B). Additional thresholds (ratios or fluorescence intensities) select species further; for example, D–A species can be selected using the sum of $F_{A_{ex}}$ and $F_{D_{ex}}$ intensities (Figure 7C).

Thresholding can also be used for one-dimensional E or S histograms. For example, the E histogram for D-only and D–A complexes essentially reconstructs the outcome of single-laser excitation TIR microscopy (Figure 7D). Thresholding removes all D-only species, permitting E measurements even at low FRET (Figure 7E; $E \approx 0.18$) and extending the range of accessible distances.
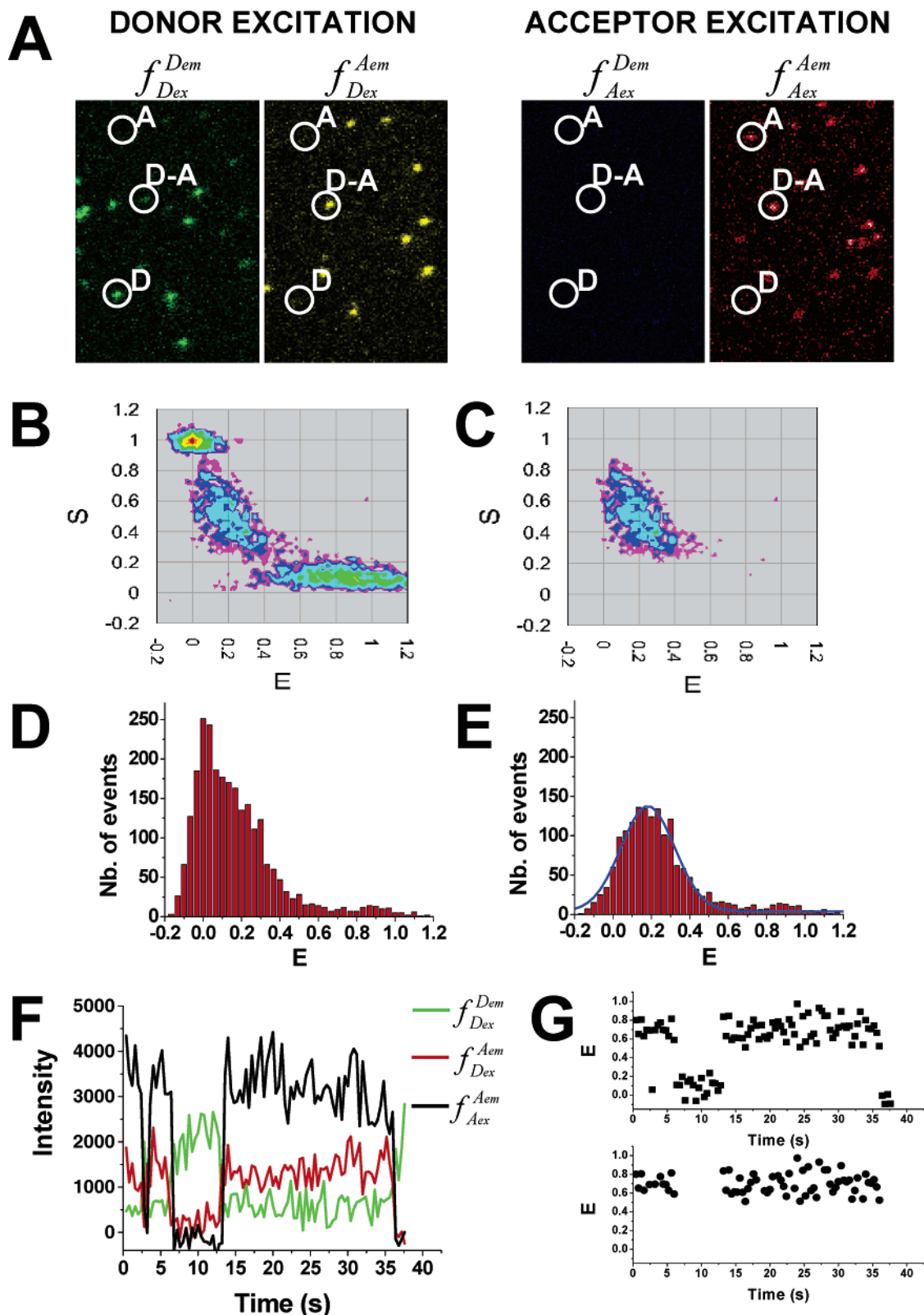
FIGURE 7. ms-ALEX microscopy. Panel A shows fluorescence from multiple immobilized complexes obtained by alternation between donor excitation (left) and acceptor excitation (right). Encircled molecules represent the main species. Panel B shows the $E-S$ histogram of a low-FRET sample containing all species. Panel C shows the $E-S$ histogram of the sample in panel B after only the D–A species are retained. Panel D shows the E-histogram for single-laser excitation TIR, showing overlap of D-only and D–A species. Panel E shows the E-histogram for ms-ALEX microscopy, after D–A species are selected (as in panel C). Panel F shows fluorescence-intensity time traces for a high-E complex, showing that increased f_{Dex}^{Dem} is due to acceptor blinking. Panel G shows FRET traces calculated from panel F: top, E calculated using the complete timetrace; bottom, E values after the time points with active acceptor are selected, thus eliminating changes in E due to acceptor blinking.

Importantly, ms-ALEX identifies and removes photophysics (e.g., fluorophore blinking) from fluorescence-intensity time traces for individual molecules (Figure 7F). Anticorrelated intensities $f_{D_{ex}}^{D_{em}}$ and $f_{D_{ex}}^{A_{em}}$ (Figure 7F, green and red curves) are used routinely in single-excitation TIR to identify FRET changes due to dynamics that change interprobe distances. However, processes that render a FRET acceptor unable to accept energy or to emit photons produce a similar observable: a transient decrease in apparent E (Figure 7F; low-E state in Figure 7G, top). In ms-ALEX, direct observation of the acceptor state using A-excitation ($f_{A_{ex}}^{A_{em}}$ signal; Figure 7F, black curve) shows clearly that the specific FRET change is due to acceptor blinking. Thus, by selecting parts of the time trace wherein the acceptor is active (using a $f_{A_{ex}}^{A_{em}}$ threshold), we can generate blinking-free E traces (Figure 7G, bottom), allowing conformational transitions to be observed without complications. Using this "photophysics sorting", we studied dynamics during promoter escape by RNAP. Similar analysis that monitors transient S changes can detect multiround loading/unloading of biomolecules on immobilized templates.

Nanosecond-ALEX: Searching for Fast Dynamics

Interlacing two pulsed lasers (D_{exc} and A_{exc}; picosecond pulses) with a fixed time delay between pulses achieves alternating-laser excitation while monitoring donor and acceptor fluorescence lifetimes (nanosecond time scale). Two time measurements are made for each photon: the time since the experiment began (macrotime t; Figure 8A) and the time delay between a D_{exc} pulse and a photon (microtime τ; Figure 8B). The macrotime is used to identify single-molecule transits across the observation volume and to form correlations and time traces; the microtime is used to determine fluorescence lifetime and assign laser excitation to a photon (by dividing photons into groups detected after D_{exc} and after A_{exc}; Figure 8B) (Lawrence et al., submitted for publication).

ALEX at the nanosecond time scale (nanosecond-ALEX or ns-ALEX) creates new capabilities for single-molecule FRET. For example, ns-ALEX allows distance measurements without detection corrections, since lifetime measurements measure FRET using only donor lifetime in the presence (τ^D) and absence (τ_0^D) of acceptor ($E = 1 - \{\tau^D/\tau_0^D\}$). Since such measurements involve a single fluorophore and detector, no detection correction is necessary.[34]

Nanosecond-ALEX can scrutinize the rotational freedom of fluorophores, setting limits for the extent that probe orientation affects a distance measurement. (FRET, in addition to its distance dependence, depends on the relative orientation of D-emission and A-excitation dipoles,[35] compounded in orientation factor κ^2, which equals $^2/_3$ for free rotation of donor and acceptor.[36] Characterization of the rotational freedom is necessary for reliable distance measurements and performed using steady-state and time-resolved fluorescence anisotropy.[37]) In ns-ALEX,
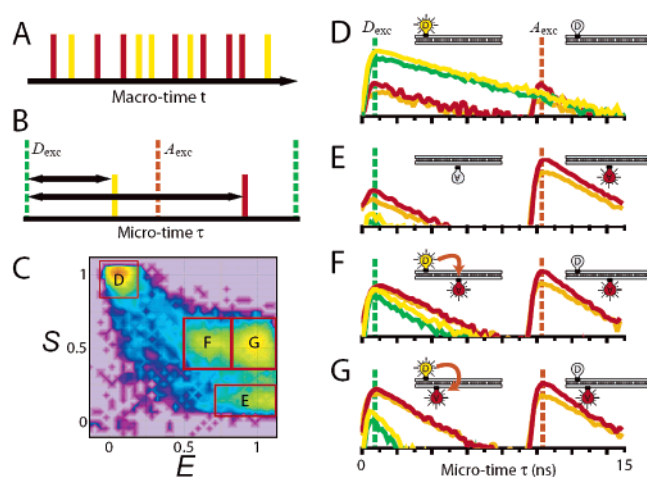
FIGURE 8. Nanosecond-ALEX. Green laser pulses (D_{exc}, dotted green lines) excite the donor, and red laser pulses (A_{exc}, dotted red lines) excite the acceptor. Fluorescence-intensity decays of donor and acceptor are shown as yellow and red curves, respectively. In panels A and B, the data obtained for each photon include the detection channel (donor, yellow line; acceptor, red line), the macrotime t, and the microtime τ (time delay between a detected photon and a laser pulse). Photons can be attributed to D_{exc} or A_{exc} depending on whether a photon with microtime τ is detected before or after the A_{exc} pulse. Panel C shows an E–S histogram formed using ns-ALEX for a sample containing four DNA fragments—D-only, A-only, intermediate-E DNA, and high-E DNA. Intensity decays are formed for sorted species (in red boxes). Gold and green decays represent donor emission parallel and perpendicular to excitation polarization, respectively. Red and orange decays represent acceptor emission parallel and perpendicular to excitation polarization, respectively. Splitting between the parallel and perpendicular polarizations indicates rotational diffusion of donor and acceptor during the fluorescence lifetime. The shortened donor lifetime in species F and G (cf. to species D) is due to FRET. In panel D, D-only species emit primarily after a green pulse (experimental decays convolved with temporal response of detectors). In panel E, A-only species emit primarily after a red pulse (weak emission after green pulse is due to direct acceptor excitation). In panel F, D–A species with intermediate FRET emit donor and acceptor fluorescence after a green pulse (with ratio of intensities and lifetimes depending on FRET) and emit acceptor fluorescence after a red pulse. In panel G, D–A species with high FRET emit primarily acceptor fluorescence after a green pulse and only acceptor fluorescence after a red pulse.

we use linearly polarized excitation and divide the fluorescence emission by polarization, as well as by spectrum, thus performing time-resolved anisotropy and FRET measurements. Lifetime measurements measure the decay of anisotropy over the 0.1–10 ns time scale, directly evaluating the rotational freedom of the fluorophores.

Lifetime measurements improve distance measurements by recovering distances that fluctuate on time scales slower than fluorescence lifetime. FRET shortens donor lifetime τ^D according to $\tau^D = \tau_0^D(1 - E)$. For a single interprobe distance, the donor-intensity decay is described by a single (shortened) lifetime. For multiple distances, one expects multiple donor lifetimes, which are difficult to recover solely from donor-intensity decays. Global analysis of donor-intensity and acceptor-intensity decays improves the accuracy of recovered distance distributions, since acceptor-intensity decays emphasize short distances

(high E; short τ^{D}), whereas donor-intensity decays emphasize long distances (low E; long τ^{D}). Distance fluctuations on the time scale of fluorescence lifetime narrow the observed distance distributions.[38]

FRET-based analysis of distance distributions using ensemble time-resolved fluorescence is obscured by the presence of multiple species, such as folded and unfolded proteins, or incomplete labeling. ns-ALEX uses single-molecule sorting to select each species (Figure 8C), obtaining lifetime histograms that include photons from only one species. Fluorescence-intensity decay analysis is typically performed for all photons from each species, since it is difficult to perform using the few photons (<100) detected from a single molecule. For each sample, diffusing molecules are sorted into species on $E-S$ histograms (Figure 8C), and fluorescence-decay plots are generated for the photons from each species (Figure 8D–G). ns-ALEX recovers all the parameters needed to describe donor- and acceptor-intensity decays. For instance, when the intensity after D_{exc} and A_{exc} for A-only species (Figure 8E) is compared, direct acceptor excitation by D_{exc} (A-direct excitation) is quantified. Donor-emission into the acceptor-detection channel (D-leakage) is similarly quantified using D-only species (Figure 8D). These corrections, along with the intrinsic acceptor lifetime after A_{exc}, quantify the crosstalk contributions of D-leakage and A-direct excitation, constraining the fitting of the acceptor decays after the D_{exc} pulse.

The end result of ns-ALEX is the simultaneous recovery of distance distributions, orientational dynamics, and accurate distances, opening new avenues for studying biomolecular structure, dynamics, and interactions.

Conclusion and Outlook

Alternating-laser excitation spectroscopy adds new tools to the single-molecule toolbox. ALEX-based sorting analyzes complex samples without strict requirements for high purity, optimal distance range, or high concentration, facilitating reagent preparation. ALEX offers the ability to perform sophisticated experiments *in solution*, enabling direct comparisons between ensemble and single-molecule assays and obviating immobilization.

Apart from the advantage of ALEX over spFRET in monitoring interactions without FRET, a salient feature of ALEX is the improved distance measurement within single molecules. Since SMFS sensitivity is high (requiring $6-10$ orders of magnitude less material than crystallography or NMR), the accurate distance capability of ALEX (with fluorophores having adequate rotational freedom), combined with rapid preparation of small amounts of labeled biomolecules, can lead to solution-based, low-resolution structures of biomolecules and their complexes, as done using ensemble-FRET and distance-restrained docking.[39] Such an approach is suitable for large, multicomponent, heterogeneous complexes of cellular machinery (especially if inaccessible to conventional structural biology), and it will benefit from existing crystallographic or NMR-based structures.

The flexibility of ALEX leaves ample room for expansion. An extension of μs-ALEX adds a third fluorophore, excitation source, and detected-emission range (three-color ALEX). For example, an SMFS-compatible,[6] fluorescein-like fluorophore complements well the common FRET pair of tetramethylrhodamine and Cy5. We demonstrated the feasibility of three-color ALEX using triply labeled DNA (N.L., A.K., and S.W., manuscript in preparation). Multicolor ALEX allows simultaneous measurements of several distances within a single molecule, allowing triangulation and construction of structural models. It also enables real-time, multiperspective views of biomachinery, since monitoring *multiple* distances and stoichiometries within a complex (such as the replisome or the ribosome) will detail the extent, kinetics, and sequence of conformational changes and assembly/disassembly events that define mechanisms of action.

ALEX can be extended to study fluorescent species in concentrations higher than 1 nM. This can be achieved by combining ALEX with correlation analysis on sorted species, recovering fluctuation time scales and associated amplitudes.[40] Methods that confine excitation volume[41] will greatly increase the upper concentration limit of ALEX. The concentration limitation (general for SMFS) can be solved by using nonfluorescent analytes, which can be present at any concentration and can monitor their effect by observing the status of the labeled species (present in picomolar concentrations)

Other extensions combine ALEX with physical sorting[42] (purifying species of interest by on-line detection of distance and stoichiometry, followed by amplification or analysis) and with observations of interactions/dynamics in living cells (pending advances in site-specific labeling[6]). Finally, ALEX-based high-throughput bioassays will result in robust biotechnology applications, such as diagnostic and drug-discovery assays.

References

(1) Moerner, W. E.; Orrit, M. Illuminating single molecules in condensed matter. *Science* **1999**, *283*, 1670–1676.
(2) Ha, T. Structural dynamics and processing of nucleic acids revealed by single-molecule spectroscopy. *Biochemistry* **2004**, *43*, 4055–4063.
(3) Weiss, S. Measuring conformational dynamics of biomolecules by single molecule fluorescence spectroscopy. *Nat. Struct. Biol.* **2000**, *7*, 724–729.
(4) Weiss, S. Fluorescence spectroscopy of single biomolecules. *Science* **1999**, *283*, 1676–1683.
(5) Michalet, X.; Kapanidis, A. N.; Laurence, T.; Pinaud, F.; Doose, S.; Pflughoefft, M.; Weiss, S. The power and prospects of fluorescence microscopies and spectroscopies. *Annu. Rev. Biophys. Biomol. Struct.* **2003**, *32*, 161–182.
(6) Kapanidis, A. N.; Weiss, S. Fluorescent probes and bioconjugation chemistries for single-molecule fluorescence analysis of biomolecules. *J. Chem. Phys.* **2002**, *117*, 10953–10964.
(7) Nie, S.; Zare, R. N. Optical detection of single molecules. *Annu. Rev. Biophys. Biomol. Struct.* **1997**, *26*, 567–596.

(8) Ha, T. Single-Molecule Fluorescence Resonance Energy Transfer. *Methods* **2001**, *25*, 78–86.

(9) Peterman, E. J.; Sosa, H.; Moerner, W. E. Single-molecule fluorescence spectroscopy and microscopy of biomolecular motors. *Annu. Rev. Phys. Chem.* **2004**, *55*, 79–96.

(10) Ambrose, W. P.; Goodwin, P. M.; Jett, J. H.; Van Orden, A.; Werner, J. H.; Keller, R. A. Single molecule fluorescence spectroscopy at ambient temperature. *Chem. Rev.* **1999**, *99*, 2929–2956.

(11) Deniz, A. A.; Laurence, T. A.; Dahan, M.; Chemla, D. S.; Schultz, P. G.; Weiss, S. Ratiometric single-molecule studies of freely diffusing biomolecules. *Annu. Rev. Phys. Chem.* **2001**, *52*, 233–253.

(12) Zhuang, X.; Rief, M. Single-molecule folding. *Curr. Opin. Struct. Biol.* **2003**, *13*, 88–97.

(13) Kulzer, F.; Orrit, M. Single-molecule optics. *Annu. Rev. Phys. Chem.* **2004**, *55*, 585–611.

(14) Eigen, M.; Rigler, R. Sorting single molecules – application to diagnostics and evolutionary biotechnology. *Proc. Natl. Acad. Sci. U.S.A.* **1994**, *91*, 5740–5747.

(15) Hess, S. T.; Huang, S.; Heikal, A. A.; Webb, W. W. Biological and chemical applications of fluorescence correlation spectroscopy: a review. *Biochemistry* **2002**, *41*, 697–705.

(16) Hirschfeld, T. Optical microscopic observation of single small molecules. *Appl. Opt.* **1976**, *15*, 2965–2966.

(17) Shera, E. B.; Seitzinger, N. K.; Davis, R. A.; Keller, R. A.; Soper, S. A. Detection of single fluorescent molecules. *Chem. Phys. Lett.* **1990**, *174*, 553–557.

(18) Michalet, X.; Lacoste, T. D.; Weiss, S. Ultrahigh-resolution colocalization of spectrally separable pointlike fluorescent probes. *Methods* **2001**, *25*, 87–102.

(19) Bruchez, M., Jr.; Moronne, M.; Gin, P.; Weiss, S.; Alivisatos, A. P. Semiconductor nanocrystals as fluorescent biological labels. *Science* **1998**, *281*, 2013–2016.

(20) Xu, C.; Zipfel, W.; Shear, J. B.; Williams, R. M.; Webb, W. W. Multiphoton fluorescence excitation: new spectral windows for biological nonlinear microscopy. *Proc. Natl. Acad. Sci. U.S.A.* **1996**, *93*, 10763–10768.

(21) Ha, T.; Ting, A. Y.; Liang, J.; Caldwell, W. B.; Deniz, A. A.; Chemla, D. S.; Schultz, P. G.; Weiss, S. Single-molecule fluorescence spectroscopy of enzyme conformational dynamics and cleavage mechanism. *Proc. Natl. Acad. Sci. U.S.A.* **1999**, *96*, 893–898.

(22) Deniz, A. A.; Dahan, M.; Grunwell, J. R.; Ha, T.; Faulhaber, A. E.; Chemla, D. S.; Weiss, S.; Schultz, P. G. Single-pair fluorescence resonance energy transfer on freely diffusing molecules: observation of Förster distance dependence and subpopulations. *Proc. Natl. Acad. Sci. U.S.A.* **1999**, *96*, 3670–3675.

(23) Li, H.; Ying, L.; Green, J. J.; Balasubramanian, S.; Klenerman, D. Ultrasensitive coincidence fluorescence detection of single DNA molecules. *Anal. Chem.* **2003**, *75*, 1664–1670.

(24) Kapanidis, A. N.; Lee, N. K.; Laurence, T. A.; Doose, S.; Margeat, E.; Weiss, S. Fluorescence-aided molecule sorting: analysis of structure and interactions by alternating-laser excitation of single molecules. *Proc. Natl. Acad. Sci. U.S.A.* **2004**, *101*, 8936–8941.

(25) Sako, Y.; Minoghchi, S.; Yanagida, T. Single-molecule imaging of EGFR signaling on the surface of living cells. *Nat. Cell Biol.* **2000**, *2*, 168–172.

(26) Braslavsky, I.; Hebert, B.; Kartalov, E.; Quake, S. R. Sequence information can be obtained from single DNA molecules. *Proc. Natl. Acad. Sci. U.S.A.* **2003**, *100*, 3960–3964.

(27) Deniz, A. A.; Laurence, T. A.; Beligere, G. S.; Dahan, M.; Martin, A. B.; Chemla, D. S.; Dawson, P. E.; Schultz, P. G.; Weiss, S. Single-molecule protein folding: diffusion fluorescence resonance energy transfer studies of the denaturation of chymotrypsin inhibitor 2. *Proc. Natl. Acad. Sci. U.S.A.* **2000**, *97*, 5179–5184.

(28) Lee, N. K.; Kapanidis, A. N.; Wang, Y.; Michalet, X.; Mukhopadhyay, J.; Ebright, R. H.; Weiss, S. Accurate FRET measurements within single diffusing biomolecules using alternating-laser excitation. *Biophys. J.* **2005**, *88*, 1–15.

(29) Norman, D. G.; Grainger, R. J.; Uhrin, D.; Lilley, D. M. J. Location of Cyanine-3 on Double-Stranded DNA: Importance for Fluorescence Energy Transfer Studies. *Biochemistry* **2000**, *39*, 6317–6324.

(30) Mukhopadhyay, J.; Kapanidis, A. N.; Mekler, V.; Kortkhonjia, E.; Ebright, Y. W.; Ebright, R. H. Translocation of sigma(70) with RNA polymerase during transcription: fluorescence resonance energy transfer assay for movement relative to DNA. *Cell* **2001**, *106*, 453–463.

(31) Axelrod, D. Total internal reflection fluorescence microscopy in cell biology. *Traffic* **2001**, *2*, 764–774.

(32) Ha, T.; Rasnik, I.; Cheng, W.; Babcock, H. P.; Gauss, G. H.; Lohman, T. M.; Chu, S. Initiation and re-initiation of DNA unwinding by the *Escherichia coli* Rep helicase. *Nature* **2002**, *419*, 638–641.

(33) Kinosita, K.; Itoh, H.; Ishiwata, S.; Hirano, K.; Nishizaka, T.; Hayakawa, T. Dual-view microscopy with a single camera – real-time imaging of molecular orientations and calcium. *J. Cell Biol.* **1991**, *115*, 67–73.

(34) Rothwell, P. J.; Berger, S.; Kensch, O.; Felekyan, S.; Antonik, M.; Wohrl, B. M.; Restle, T.; Goody, R. S.; Seidel, C. A. Multiparameter single-molecule fluorescence spectroscopy reveals heterogeneity of HIV-1 reverse transcriptase:primer/template complexes. *Proc. Natl. Acad. Sci. U.S.A.* **2003**, *100*, 1655–1660.

(35) Clegg, R. M. Fluorescence resonance energy transfer and nucleic acids. *Methods Enzymol.* **1992**, *211*, 353–388.

(36) Lakowicz, J. R. *Topics in Fluorescence Spectroscopy*; Plenum Press: New York, 1991; Vol. 2.

(37) Kapanidis, A. N.; Ebright, Y. W.; Ludescher, R. D.; Chan, S.; Ebright, R. H. Mean DNA bend angle and distribution of DNA bend angles in the CAP-DNA complex in solution. *J. Mol. Biol.* **2001**, *312*, 453–468.

(38) Beechem, J. M.; Haas, E. Simultaneous determination of intramolecular distance distributions and conformational dynamics by global analysis of energy transfer measurements. *Biophys. J.* **1989**, *115*, 1225–1236.

(39) Mekler, V.; Kortkhonjia, E.; Mukhopadhyay, J.; Knight, J.; Revyakin, A.; Kapanidis, A. N.; Niu, W.; Ebright, Y. W.; Levy, R.; Ebright, R. H. Structural organization of bacterial RNA polymerase holoenzyme and the RNA polymerase-promoter open complex. *Cell* **2002**, *108*, 599–614.

(40) Doose, S.; Tsay, J. M.; Pinaud, F.; Weiss, S. Comparison of photophysical and colloidal properties of biocompatible semiconductor nanocrystals using fluorescence correlation spectroscopy. *Anal. Chem.* **2005**, ASAP, DOI 10.1021/ac050035n.

(41) Laurence, T. A.; Weiss, S. Analytical chemistry. How to detect weak pairs. *Science* **2003**, *299*, 667–668.

(42) Dittrich, P. S.; Schwille, P. An integrated microfluidic system for reaction, high-sensitivity detection, and sorting of fluorescent cells and particles. *Anal. Chem.* **2003**, *75*, 5767–5774.